Received: 8 March 2018 | Revised: 17 September 2018 | Accepted: 17 November 2018

DOI: 10.1002/rnc.4432

RESEARCH ARTICLE

WILEY

Robust event-triggered model predictive control for constrained linear continuous system

Yu Luo | Yuanqing Xia | Zhongqi Sun

School of Automation, Beijing Institute of Technology, Beijing, China

Correspondence
Yuanqing Xia, School of Automation, Beijing Institute of Technology, Beijing 100081, China.
Email: xia_yuanqing@bit.edu.cn

Funding information
Beijing Natural Science Foundation, Grant/Award Number: 4161001; National Natural Science Foundation, Grant/Award Number: 61836001 and 61803033; National Natural Science Foundation Projects of International Cooperation and Exchanges, Grant/Award Number: 61720106010; Foundation for Innovative Research Groups of the National Natural Science Foundation of China, Grant/Award Number: 61621063

Summary

Model predictive control (MPC) is capable to deal with multiconstraint systems in real control processes; however, the heavy computation makes it difficult to implement. In this paper, a dual-mode control strategy based on event-triggered MPC (ETMPC) and state-feedback control for continuous linear time-invariant systems including control input constraints and bounded disturbances is developed. First, the deviation between the actual state trajectory and the optimal state trajectory is computed to set an event-triggered mechanism and reduce the computational load of MPC. Next, the dual-mode control strategy is designed to stabilize the system. Both recursive feasibility and stability of the strategy are guaranteed by constructing a feasible control sequence and deducing the relationship of parameters, especially the inter-event time and the upper bound of the disturbances. Finally, the theoretical results are supported by numerical simulation. In addition, the effects of the parameters are discussed by simulation, which gives guidance to balance computational load and control performance.

KEYWORDS

bounded disturbances, continuous LTI system, event-triggered, input constraints, model predictive control

1 | INTRODUCTION

Receding horizon control, or model predictive control (MPC), can handle multiple-input–multiple-output complex systems with hard control constraints easily and effectively. This has inspired many research efforts into the field in recent years.[1] By solving a finite horizon, constrained, discrete-time, open-loop optimal control problem at each sampling instant, a control sequence is obtained. The first control input of the sequence is applied to the plant at the current state and the process is repeated, which provides an effective way to approximate the optimal solution.[2,3] In the real control process with constraints and disturbances, MPC provides a suitable method to overcome the potential performance degradation and stability problems.[4-7]

In published literatures on MPC, there are many instructive results to reduce the impacts of uncertainty and disturbances. Bemporad and Morari,[8] gave an overview of robustness for MPC and proposed some techniques for robust constraints handling, stability, and performance guarantee. By using the notion of tubes in other works,[9-11] or by comparing nominal MPC performance cost shown in the works of Ding et al[12] and Marruedo et al,[13] the robustness of the controller can be ensured.

Due to solving an optimization problem at each sampling instant and using only the first control input of the optimal control sequence, conventional time-triggered MPC requires relatively heavy computational load compared with other controllers,[2] which brings difficulties for implementing the controller to the real system. To improve utilization of the control sequence and reduce the computational load, aperiodic control which has several significant performance advantages in explicitly addressing energy, computation, and communication constraints is of increasing concern.[14] An event-triggered mechanism is one of the aperiodic control techniques, which updates new control actuation when the predefined condition is violated.[15,16] In the work of Lunze and Lehmann,[17] by deriving an upper bound of the difference between the continuous state-feedback loop and the event-based control loop, a new method for event-based state-feedback control was developed, giving a framework of event-triggered control. Heemels and Donkers[18] combined conventional periodic sampled-data control with event-triggered control to design periodic event-triggered control.

Combined with event-triggered mechanism, robust MPC can obtain satisfactory performance and reduce computational load compared with conventional MPC.[19-21] In the work of Ferrara et al,[22] an efficient control framework for freeway systems was developed based on MPC, and the control law was updated when the considered error exceeded a predefined threshold. The focus of Lehmann et al[7] lied in ETMPC for discrete-time linear systems, where robust feasibility and stability were discussed in detail. In the work of Brunner et al,[23] by designing event-triggered conditions, the average frequency of communication was reduced and the robustness was ensured by tube MPC. Li and Shi,[24] combined the event-triggered mechanism and robust MPC to apply to nonlinear systems, which gave a comprehensive approach to reduce computational load and guarantee the stability.

Similar to the event-triggered mechanism, the next triggering time is precomputed at current sampling instant based on the current system state and system dynamics in the self-triggered mechanism.[25,26] Brunner et al[27] proposed a robust self-triggered control algorithm with tube MPC for constrained linear discrete-time systems subject to additive disturbances, which gave an effective way of robustifying MPC and reduced communication and computational load. By the min-max MPC framework and the self-triggered strategy, the authors designed a novel cost function and developed the feasibility and the closed-loop stability of the algorithm in the work of Liu et al.[28] In the work of Hashimoto et al,[29] MPC with self-triggered formulation was established for continuous-time nonlinear input-affine networked control systems, which gave the stability analysis under the sample-and-hold implementation. However, there are few literatures about constrained continuous system with robust ETMPC. Moreover, compared with nonlinear systems, linear time-invariant (LTI) systems, which can always obtain an analytical solution, are suitable for ETMPC to reduce conservatism.

In this paper, a dual-mode control strategy for the LTI continuous systems with input constraints and bounded disturbances is proposed. Nominal MPC performance cost with the upper bound of the disturbances is chosen to substitute the "worst case" to achieve robustness. By designing an event-triggered mechanism, the computational load is observably reduced while recursive feasibility and stability are guaranteed. The main contributions of the paper are summarized as follows:

1. A dual-mode control strategy is designed by ETMPC and state-feedback control law to stabilize the system. By setting a threshold between the real state trajectory and the optimal state trajectory, event-triggered mechanism is introduced to reduce the computational load.
2. To apply the dual-mode strategy to the real system, a robust terminal region and the parameters of the strategy are designed for the optimization problem to obtain recursive feasibility and stability. In the numerical simulation, the effects of the inter-event time and the upper bound of the disturbances are discussed in detail.

The rest of this paper is organized as follows. In Section 2, the system model with input constraints and bounded disturbances is built and the optimization problem is formulated. Section 3 presents that the dual-mode control strategy is designed based on the event-triggered mechanism and robust MPC. Recursive feasibility and stability are analyzed in Section 4. In Section 5, numerical simulation validates the theoretical results and the effects of parameters are presented. The conclusion is shown in Section 6.

In order to simplify the representations of variables with different meanings, we adopt some labels and special symbols as follows. The natural integers are denoted by $\mathbb{N}$, and $\mathbb{R}$ denotes the real numbers. For the state and control variables, the ones solved by the optimization problems are represented as $\cdot^*$ and the ones which provide a feasible solution and satisfy all of constraints are represented as $\bar{\cdot}$. For the matrix P, $\overline{\lambda}(P)$ and $\underline{\lambda}(P)$ denote the largest and the smallest real part of the eigenvalues of P, respectively. $\sqrt{P}$ is Cholesky factorization which means $P = (\sqrt{P})^T\sqrt{P}$. If P is Hurwitz, all eigenvalues of P have a strictly negative real part. At last, $\|x\|_P$ is p-norm of x which is defined as $\sqrt{x^TPx}$ and $\|x\|$ is 2-norm of x as $\sqrt{x^Tx}$.

2 | PROBLEM FORMULATION

In this section, we describe the model of a continuous LTI system with bounded disturbances and constraints and formulate the optimization problem. Consider a system model as

$$\dot{x}(t) = Ax(t) + Bu(t) + E\omega(t),\ x(t_0) = x_0,\ t_0 \geqslant 0, \tag{1}$$

where $x(t) \in \mathbb{R}^n$ is the system state, and $u(t) \in \mathbb{R}^m$ is the control input. In the model, the control input is subject to $u(t) \in \mathcal{U}$. $\omega(t) \in \mathcal{W} \subset \mathbb{R}^l$ is a unknown disturbance which is bounded by $\eta = \sup_{\omega(t)\in\mathcal{W}}\|\omega(t)\|$. $A \in \mathbb{R}^{n\times n}$, $B \in \mathbb{R}^{n\times m}$, and $E \in \mathbb{R}^{n\times l}$ are time-invariant matrices. In addition, both the state and the control input feasible region are convex and compact including the origin as an interior point. For the disturbance, we only suppose that the disturbance has an upper bound η.

For system (1), a fundamental assumption is necessary: if $\omega(t) = 0$ is satisfied, the system can be stabilizable by appropriate control input.[30] According to this assumption and the technique of state-feedback control, we acquire a state-feedback gain K for the system as $u = Kx$. Then, the state-space model can be rewritten as

$$\dot{x}(t) = (A + BK)x(t) + E\omega(t). \tag{2}$$

To ensure the stability of the system with disturbances, we give a lemma to describe the convergence domain of the system.

Lemma 1. *For system (2), there exists a state-feedback gain K, which satisfies that $A + BK$ is Hurwitz and the control input $u = Kx$ meets the constraint $u \in \mathcal{U}$ when the state trajectory converges in a certain time-invariant region. Then, the closed-loop system is stable. Furthermore, the region is defined as a time-invariant set $\Omega_\gamma = \{x|\|x\| \leqslant \gamma\}$, where*

$$\gamma = \left\| \lim_{\tau\to+\infty} \int_{t_0}^{\tau} e^{(A+BK)(\tau-s)} E\eta ds \right\|. \tag{3}$$

Remark 1. Lemma 1 implies that the system has at least one feasible and simple solution to ensure the state variables stabilizable. However, in most practical control process with input constraint, $u = Kx$ hardly satisfies the constraint $u(t) \in \mathcal{U}$. Thus, we consider a dual-mode control law to solve this problem. If $u = Kx$ does not meet the constraint, we apply MPC to obtain the optimal control sequence; otherwise, we use the state-feedback control law for conciseness. Furthermore, by constructing a Lyapunov function, we verify that once $x(t)$ enters the Ω_γ, the state will be practically stable and the radius of convergence domain depends on the upper bound of the disturbance.

Remark 2. To improve practicability, the terminal region for MPC should be as wide as possible to apply $u = Kx$ as soon as possible. In this article, we design a terminal set Ω_r and a robust terminal set Ω_ϵ in the following parts while Ω_γ is a convergence domain to show the practical stability.

For system (1), define T as the prediction horizon. At each sampling instant t_k, $k \in \mathbb{N}$, we consider the following optimization problem (4)-(5), which is formulated as

$$\min_{\bar{u}(\tau|t_k)\in\mathcal{U}} \quad J(t_k, \bar{x}(\tau|t_k), \bar{u}(\tau|t_k)), \tag{4}$$

subject to

$$\begin{aligned} \dot{\bar{x}}(\tau|t_k) &= A\bar{x}(\tau|t_k) + B\bar{u}(\tau|t_k), \\ \bar{x}(t_k|t_k) &= x(t_k),\ \|\bar{x}(t_k + T|t_k)\| \in \Omega_\varepsilon, \\ \|\bar{x}(\tau|t_k)\| &\leqslant \frac{T\varepsilon}{\tau - t_k},\ \tau \in (t_k, t_k + T], \\ \bar{u}(\tau|t_k) &\in \mathcal{U},\ \tau \in (t_k, t_k + T], \end{aligned} \tag{5}$$

where $J(t_k, \bar{x}(\tau|t_k), \bar{u}(\tau|t_k))$ is the optimization cost function, $\Omega_\varepsilon = \{x|\|x(t)\| \leqslant \varepsilon\}$ is the robust terminal region and ε is a designed constant. By solving the problem, the optimal control input is obtained as $u^*(\tau|t_k)$.

In the problem, the cost function is defined as

$$J(t_k, \bar{x}, \bar{u}) = \int_{t_k}^{t_k+T} L(\tau|t_k, \bar{x}, \bar{u})d\tau + g(\bar{x}(t_k + T|t_k)), \tag{6}$$

where $L(\tau|t_k,\bar{x},\bar{u}) = \|\bar{x}(\tau|t_k)\|_Q^2 + \|\bar{u}(\tau|t_k)\|_R^2$ is the stage cost, $g(\bar{x}(t_k+T|t_k)) = \|\bar{x}(t_k+T|t_k)\|_P^2$ is the terminal penalty function, and Q, R, and P are Hermitian positive-define matrices.

3 | EVENT-TRIGGERED MECHANISM

For the time-triggered MPC, we need to solve the optimization problem at each sampling instant t_k, which brings complex operations and slow response. As stated in the *Introduction* section, aperiodic control, especially the event-triggered mechanism, can deal with the computational load caused by MPC. In this section, the event-triggered mechanism is designed to combine with MPC. The key of event-triggered mechanism is to set a threshold value as the upper bound of the difference between the optimal state trajectory and the real one. The following lemma indicates that the trajectory difference depends on the prediction time $\tau - t_k$ and the upper bound of the disturbances η, where $\tau \in [t_k, t_k+T]$.

Lemma 2. *For $\tau \in [t_k, t_k+T]$, under the same optimal control input $u^*(\tau|t_k)$, the difference between the optimal state trajectory and the real one is bounded by*

$$\|x^*(\tau|t_k) - x(\tau)\| \leqslant \vartheta(\tau - t_k), \tag{7}$$

where $\vartheta(s) = me^{as} - m$, $m = \frac{\eta\|E\|}{\|A\|}$, and $a = \|A\|$.

Proof. According to the solution of the time-invariant linear equation (see the work of Zadeh and Deoser[31]), matrix inequality, and the actual state $x(t_k) = x^*(t_k|t_k)$, we have

$$\begin{aligned}
\|x(\tau) - x^*(\tau|t_k)\| &= \Big\| e^{A(\tau-t_k)}x(t_k) + \int_{t_k}^{\tau} e^{A(\tau-s)}(Bu^*(s) + E\omega(s))ds \\
&\quad - e^{A(\tau-t_k)}x^*(t_k|t_k) - \int_{t_k}^{\tau} e^{A(\tau-s)}Bu^*(s)ds \Big\| \\
&= \left\| \int_{t_k}^{\tau} e^{A(\tau-s)}E\omega(s)ds \right\| \\
&\leqslant \int_{t_k}^{\tau} e^{\|A\|(\tau-s)}\|E\|\eta ds \\
&= \frac{\eta\|E\|}{\|A\|}e^{\|A\|(\tau-t_k)} - \frac{\eta\|E\|}{\|A\|} \\
&= \vartheta(\tau - t_k),
\end{aligned}$$

where $\tau \in [t_k, t_k+T]$. □

Remark 3. The proof is based on the solution of the continuous LTI system and the inequalities of matrix norms. In the work of Li and Shi,[24] the state trajectory difference is deduced by the Gronwall-Bellman inequality and the triangle inequality because the solution of the nonlinear system can not be solved directly. Here, if we follow the method of Li and Shi,[24] the state trajectory difference is

$$\|x^*(\tau|t_k) - x(\tau)\|_P \leqslant \eta\bar{\lambda}\left(\sqrt{P}\right)(\tau - t_k)e^{\|A\|(\tau-t_k)}.$$

Moreover, in the section *Feasibility Analysis* of Li and Shi,[24] the upper bound of the disturbance is defined as

$$\eta_{[21]} = \frac{(1-\alpha)\varepsilon}{Te^{\|A\|T}\beta\bar{\lambda}(\sqrt{P})},$$

which can be compared with Theorem 1 in this paper. Hence, the solution of the continuous LTI system can reduce conservatism and permit stronger disturbance in real control process. The design and analysis of the following dual-mode control strategy are also developed by (7).

As stated in Lemma 2, under the same input, there exists a trajectory difference due to the inescapable disturbance. When the upper bound of the disturbances is certain, the upper bound of $\|x^*(\tau|t_k) - x(\tau)\|$ is an increasing function of the predict time $\tau - t_k$. As a result, the event-triggered mechanism provides an artificial appropriate upper bound of the difference to reduce the computational load and stabilize state variables. Based on the difference, we can set a threshold

value named the inter-event time σ. When the difference increases and reaches the bound $\vartheta(\sigma)$ determined by σ, the optimization problem is solved, and the optimal control sequence is updated. The event-triggered mechanism is designed as follows:

$$\|x(\tau) - x^*(\tau|t_k)\| \geqslant \vartheta(\sigma). \tag{8}$$

The Zeno behavior, which leads to an accumulation point with arbitrarily small inter-event time, should be avoided on a digital platform. To avoid this problem in the event-triggered mechanism, the inter-event time σ needs to satisfy the following inequality:

$$\Delta t \leqslant \sigma \leqslant T, \tag{9}$$

where Δt is the average sample interval. According to mechanism (8), the trajectory difference satisfies $\|x(\tau) - x^*(\tau|t_k)\| = \vartheta(\sigma)$ at the next triggering instant where $\tau \in (t_k, t_k + T]$, ie, t_{k+1} is defined as

$$t_{k+1} \geqslant \sigma + t_k. \tag{10}$$

The following inequality generalizes the relationship of the inter-event time σ:

$$\Delta t \leqslant \sigma \leqslant t_{k+1} - t_k \leqslant T. \tag{11}$$

According to Lemma 1, there exists a state-feedback law $u = Kx$ to stabilize the state $x(t)$ into the time-invariant set Ω_γ. However, Ω_γ is too small to design the terminal region. We consider a robust terminal region Ω_ε for ETMPC where ε is defined at Theorem 1 to prompt $u = Kx$. Then, as Remark 1 stated, the whole control strategy is a dual-mode strategy, which means that MPC with the event-triggered mechanism is employed until the state $x(t)$ reaches the robust terminal region and the terminal controller $u = Kx$ is used for all the future time. Based on the above control sketch, the dual-mode control is described in Algorithm 1. Figure 1 shows the whole control process from the initial point to the equilibrium point.

Algorithm 1 The dual-mode control strategy

1: Initialize the parameters of the system and calculate the radius ε of the robust terminal set.
2: **if** $x(\tau) \in \Omega_\varepsilon$ **then**
3: apply the control law $u = Kx$
4: **else**
5: solve the MPC problem of (4)
6: **while** $(\|x^*(\tau|t_k) - x(\tau)\| \leqslant \vartheta(\sigma))$ **do**
7: apply the control input calculated at t_k
8: **end while**
9: $k = k + 1$
10: **end if**
11: Update the system state $x(\tau)$ and go to step 2 .

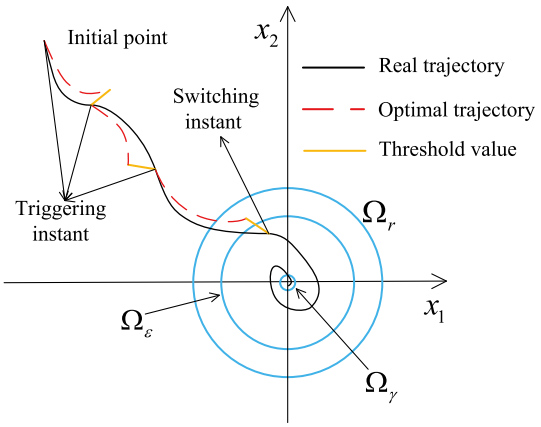

FIGURE 1 The control process of the dual-mode algorithm [Colour figure can be viewed at wileyonlinelibrary.com]

4 | ANALYSIS OF STRATEGY

For the nominal system, ie, $\dot{x} = Ax + Bu$, we apply the dual-mode strategy and design an invariant terminal region $\Omega_r = \{x | \|x(t)\| \leqslant r\}$. The following lemma gives the definition of the radius r. In addition, due to the unknown and inevitable disturbance in the real system, the robust terminal region Ω_ε for the real system belongs to Ω_r, ie, $\Omega_\varepsilon \subseteq \Omega_r$.

Lemma 3. *For the terminal region of the nominal system, the region requires (i) the radius r of the terminal region Ω_r guarantees that $\forall x \in \Omega_r$, $\exists K$, then $u = Kx$ satisfies the constraint $u \in \mathcal{U}$; (ii) the weight matrixes Q, R, and P are Hermitian positive-define matrices, which satisfy $Q + K^T RK + (A + BK)^T P + P(A + BK) \leqslant 0$, so $\forall \tau \in [t_k + T, t_{k+1} + T]$,*

$$\dot{g}\left[\bar{x}(\tau | t_k + T)\right] + L\left(\tau | t_k + T, \bar{x}, \bar{u}\right) \leqslant 0, \tag{12}$$

is guaranteed.

Proof. For the nominal system, we choose the state-feedback law $u = Kx$ as the terminal controller. Due to the input constraints and disturbances in the real system, the radius r of the terminal set is bigger than ε but bounded. For simplicity, one of feasible value of r can be considered as $r = \frac{U}{\|K\|}$, where U is the supremum of $u(t)$. In the terminal region Ω_r, by the definition of the stage cost function $L(\tau | t_k, \bar{x}, \bar{u}) = \|\bar{x}(\tau | t_k)\|_Q^2 + \|\bar{u}(\tau | t_k)\|_R^2$, the terminal penalty function $g(\bar{x}(t_k + T | t_k)) = \|\bar{x}(t_k + T | t_k)\|_P^2$ and the control law $u = Kx$, we have

$$\begin{aligned} L\left(\tau | t_k + T, \bar{x}, \bar{u}\right) + \dot{g}\left(\bar{x}(\tau | t_k + T)\right) &= \bar{x}^T Q \bar{x} + \bar{u}^T R \bar{u} + \dot{\bar{x}}^T P \bar{x} + \bar{x}^T P \dot{\bar{x}} \\ &= \bar{x}^T Q \bar{x} + \bar{x}^T K^T R K \bar{x} + \bar{x}^T (A + BK)^T P \bar{x} + \bar{x}^T P (A + BK) \bar{x} \\ &= \bar{x}^T \left[Q + K^T R K + (A + BK)^T P + P(A + BK)\right] \bar{x} \\ &\leqslant 0. \end{aligned}$$

Furthermore, by the control law $u = Kx$ and Lyapunov function, the terminal penalty function $\dot{g}(\bar{x}(\tau | t_k + T)) \leqslant -\|\bar{x}(\tau | t_k + T)\|_{Q^*}^2$, where $Q^* = Q + K^T RK$. Therefore, we can easily obtain the stability of the system in the terminal region Ω_r (see the work of Li and Shi[32]). □

4.1 | Feasibility analysis

The existence of the disturbances may cause recursive feasibility of the dual-mode strategy to be lost at each sampling instant t_k, where $k \in \mathbb{N}$. The following theorem is developed to analyze the feasibility by designing parameters of the system.

Theorem 1. *For a class of continuous LTI systems with input constraints and bounded disturbances (1), suppose that the event-triggered mechanism is defined as (8). By applying the dual-mode control strategy defined as Algorithm 1, the system has a feasible solution to converge to the robust terminal region Ω_ε, if*

i. the optimization problem has a feasible solution at the initial time t_0;
ii. the parameters of the system satisfy

1. $\eta \leqslant \frac{a(r-\varepsilon)}{\|E\|(e^{aT} - e^{a(T-\sigma)})}$, *where* $a = \|A\|$,
2. $\sigma \geqslant \frac{2\bar{\lambda}(P)}{\underline{\lambda}(Q^*)} \ln(\frac{r}{\varepsilon})$, *where* $Q^* = Q + K^T RK$,
3. $\beta r \leqslant \varepsilon \leqslant r$, *where* $\beta = \max\left\{\frac{T-\sigma}{T}, \frac{2\bar{\lambda}(P)}{T\underline{\lambda}(Q^*)}\right\}$ *and the latter satisfies* $\frac{2\bar{\lambda}(P)}{T\underline{\lambda}(Q^*)} < 1$.

Then, the dual-mode control strategy is feasible for the system.

Proof. Suppose that the system has an optimal solution at time t_k, ie, where $\tau \in [t_k, t_k + T]$, we can compute an optimal control sequence $u^*(\tau | t_k)$ by solving the optimization problem. Then, constructing a feasible solution at time t_{k+1} as follows:

$$\bar{u}(\tau | t_{k+1}) = \begin{cases} u^*(\tau | t_k), & \tau \in [t_{k+1}, t_k + T], \\ u^\kappa(\tau | t_k), & \tau \in [t_k + T, t_{k+1} + T], \end{cases} \tag{13}$$

where $u^\kappa(\tau | t_k) = Kx(\tau | t_k)$ is the state-feedback control law. Here, we give the following sketch to show the relationship between $\bar{u}(\tau | t_{k+1})$ and $u^*(\tau | t_k)$ and ensure the feasibility of $\bar{u}(\tau | t_{k+1})$ (see Figure 2).

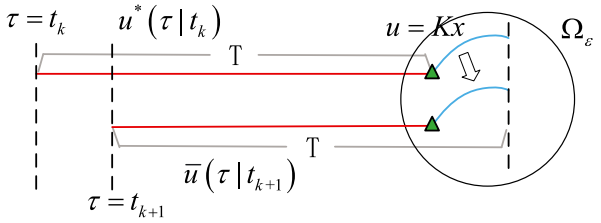

FIGURE 2 The relationship of $\bar{u}(\tau|t_{k+1})$ and $u^*(\tau|t_k)$ [Colour figure can be viewed at wileyonlinelibrary.com]

Consider the interval $\tau \in [t_{k+1}, t_k + T]$. By applying the feasible solution $\bar{u}(\tau|t_{k+1})$, we compute the difference between the feasible state trajectory and the optimal one as $\|\bar{x}(\tau|t_{k+1}) - x^*(\tau|t_k)\| = \|e^{A(\tau-t_{k+1})}x(t_{k+1}) + \int_{t_{k+1}}^{\tau} e^{A(\tau-s)}B\bar{u}(s|t_{k+1})ds - e^{A(\tau-t_{k+1})}x^*(t_{k+1}|t_k) - \int_{t_{k+1}}^{\tau} e^{A(\tau-s)}B\bar{u}(s|t_{k+1})ds\| \leqslant \|x(t_{k+1}) - x^*(t_{k+1}|t_k)\|e^{\|A\|(\tau-t_{k+1})}$. At the next sampling instant t_{k+1}, we have $\|x(t_{k+1}) - x^*(t_{k+1}|t_k)\| = \vartheta(\sigma)$ by the event-triggered mechanism. Therefore,

$$\|\bar{x}(\tau|t_{k+1}) - x^*(\tau|t_k)\| \leqslant \vartheta(\sigma)e^{\|A\|(\tau-t_{k+1})}. \tag{14}$$

Let $\tau = t_k + T$ and substitute $\vartheta(s) = me^{as} - m$ into (14), by triangle inequality and the bound of the next triggering instant $\sigma \leqslant t_{k+1} - t_k \leqslant T$, we have

$$\|\bar{x}(t_k + T|t_{k+1})\| \leqslant \|x^*(t_k + T|t_k)\| + m\left(e^{aT} - e^{a(T-\sigma)}\right). \tag{15}$$

According to the definition of the robust terminal region Ω_ε of the real system, the optimal state trajectory satisfies $\|x^*(t_k + T|t_k)\| \leqslant \varepsilon$. Substitute $\eta \leqslant \frac{\|A\|(r-\varepsilon)}{\|E\|(e^{aT}-e^{a(T-\sigma)})}$ into (15),

$$\begin{aligned}\|\bar{x}(t_k + T|t_{k+1})\| &\leqslant \varepsilon + \frac{\eta\|E\|}{\|A\|}\left(e^{aT} - e^{a(T-\sigma)}\right)\\ &\leqslant \varepsilon + r - \varepsilon\\ &= r.\end{aligned} \tag{16}$$

The proof above indicates that when the nominal system has an optimal control sequence at time t_k to make the system converge to the robust terminal set Ω_ε at time $t_k + T$ by Lemma 3, the feasible solution $\bar{u}(\tau|t_{k+1})$ constructed at time t_{k+1} can drive it into the terminal region Ω_r at the same time. Then, we need to prove that the nominal system can converge into the robust terminal region by $\bar{u}(\tau|t_k) = u^\kappa(\tau|t_k)$ where $\tau \in [t_k + T, t_{k+1} + T]$.

According to Lemma 3, the terminal penalty function satisfies $\dot{g}[\bar{x}(\tau|t_k + T)] \leqslant -\|\bar{x}(\tau|t_k + T)\|^2_{Q^*}$, where $Q^* = Q + K^TRK$. Applying the comparison principle(see the work of Khalil and Grizzle[33]), where $\tau \in [t_k + T, t_{k+1} + T]$, we have

$$g[\bar{x}(\tau|t_{k+1})] \leqslant g[\bar{x}(t_k + T|t_{k+1})]\, e^{-\frac{\lambda(Q^*)}{\bar{\lambda}(P)}(\tau-t_k-T)}. \tag{17}$$

Consider the state constraint $\bar{x}(t_k + T|t_{k+1}) \leqslant r$ and substitute $\tau = t_{k+1} + T$ into (17), then we have

$$\begin{aligned}\|\bar{x}(t_{k+1} + T|t_{k+1})\| &\leqslant re^{-\frac{\lambda(Q^*)}{2\bar{\lambda}(P)}(t_{k+1}-t_k)}\\ &\leqslant re^{-\frac{\lambda(Q^*)}{2\bar{\lambda}(P)}\sigma}.\end{aligned} \tag{18}$$

If $\sigma \geqslant \frac{2\bar{\lambda}(P)}{\lambda(Q^*)}\ln\left(\frac{r}{\varepsilon}\right)$, it indicates that $\|\bar{x}(t_{k+1} + T|t_{k+1})\| \leqslant \varepsilon$, ie, by the feasible control sequence $\bar{u}(\tau|t_{k+1})$, we can drive the feasible trajectory to enter the robust terminal region at $t_{k+1} + T$. Then, the following part proves that the feasible control sequence holds the state constraint $\|\bar{x}(\tau|t_{k+1})\| \leqslant \frac{T\varepsilon}{\tau-t_{k+1}}$.

According to (16), we apply the constraint $\|x^*(\tau|t_k)\| \leqslant \frac{T\varepsilon}{\tau-t_k}$ where $\tau \in [t_{k+1}, t_k + T]$, then $\|\bar{x}(\tau|t_{k+1})\| \leqslant \frac{T\varepsilon}{\tau-t_k} + r - \varepsilon$. Let $\beta = \frac{T-\sigma}{T}$ and because of $\beta r \leqslant \varepsilon \leqslant r$, we have $r - \varepsilon \leqslant r - \frac{T-\sigma}{T}r = \frac{\sigma}{T}r \leqslant \frac{\sigma}{T-\sigma}\varepsilon$. Considering the definition and the bound of the inter-event time σ in (11), we have $\frac{\sigma}{T-\sigma}\varepsilon \leqslant \frac{t_{k+1}-t_k}{T(T-\sigma)}T\varepsilon \leqslant \frac{t_{k+1}-t_k}{(\tau-t_{k+1})(\tau-t_k)}T\varepsilon$. Substitute the result into the

feasible state trajectory

$$\begin{aligned}\|\bar{x}(\tau|t_{k+1})\| &\leqslant \frac{T\varepsilon}{\tau - t_k} + r - \varepsilon \\ &\leqslant \frac{T\varepsilon}{\tau - t_k} + \frac{t_{k+1} - t_k}{(\tau - t_{k+1})(\tau - t_k)} T\varepsilon \\ &= \frac{\varepsilon T}{\tau - t_{k+1}},\end{aligned} \tag{19}$$

and we obtain the recursive feasibility of the state constraint in $\tau \in [t_{k+1}, t_k + T]$.

When $\tau \in [t_k + T, t_{k+1} + T]$, in terms of (17), we have $\|\bar{x}(\tau|t_{k+1})\| \leqslant re^{-\frac{\underline{\lambda}(Q^*)}{\bar{\lambda}(P)}\left(\frac{\tau - t_k - T}{2}\right)}$. If the state constraint holds, ie, the inequality above needs to satisfy $re^{-\frac{\underline{\lambda}(Q^*)}{\bar{\lambda}(P)}\left(\frac{\tau - t_k - T}{2}\right)} \leqslant \frac{\varepsilon T}{\tau - t_{k+1}}$, we can get the whole recursive feasibility. Therefore, we transform the inequality into $\frac{r(\tau - t_{k+1}) - e^{\frac{\underline{\lambda}(Q^*)}{\bar{\lambda}(P)}\left(\frac{\tau - t_k - T}{2}\right)} \varepsilon T}{e^{\frac{\underline{\lambda}(Q^*)}{\bar{\lambda}(P)}\left(\frac{\tau - t_k - T}{2}\right)} (\tau - t_{k+1})} \leqslant 0$. The denominator is verified to be positive easily, and we define

$$F(\tau) = r(\tau - t_{k+1}) - e^{\frac{\underline{\lambda}(Q^*)}{\bar{\lambda}(P)}\left(\frac{\tau - t_k - T}{2}\right)} \varepsilon T. \tag{20}$$

By differentiating $F(\tau)$, we have

$$\frac{dF}{d\tau} = r - \varepsilon T \frac{\underline{\lambda}(Q^*)}{2\bar{\lambda}(P)} e^{\frac{\underline{\lambda}(Q^*)}{\bar{\lambda}(P)}\left(\frac{\tau - t_k - T}{2}\right)}. \tag{21}$$

Let $\tau = t_k + T$ and $\beta = \frac{T - \sigma}{T}$. Since $\beta r \leqslant \varepsilon$, we easily obtain $F(t_k + T) = r(T + t_k - t_{k+1}) - \varepsilon T \leqslant r(T - \sigma) - \varepsilon T \leqslant 0$. If $F(\tau)$ is a decreasing function, we have $F(\tau) \leqslant 0$ where $\tau \in [t_k + T, t_{k+1} + T]$ and the proof is completed. By differentiating $\dot{F}(\tau)$, $\dot{F}(\tau)$ is also a decreasing function. Therefore,

$$\dot{F}(\tau)_{\max} = \dot{F}(t_k + T) = r - \varepsilon T \frac{\underline{\lambda}(Q^*)}{2\bar{\lambda}(P)} \leqslant 0. \tag{22}$$

If $\varepsilon \geqslant \frac{2\bar{\lambda}(P)}{T\underline{\lambda}(Q^*)} r$ with $\frac{2\bar{\lambda}(P)}{T\underline{\lambda}(Q^*)} < 1$, we arrive $F(\tau) \leqslant 0$ where $\tau \in [t_k + T, t_{k+1} + T]$.

As a result, the state constraint $\|\bar{x}(\tau|t_{k+1})\| \leqslant \frac{\varepsilon T}{\tau - t_{k+1}}$ is guaranteed by the feasible control sequence $\bar{u}(\tau|t_{k+1})$. The proof of recursive feasibility is completed. □

Remark 4. Theorem 1 discusses the case $\sigma \leqslant t_{k+1} - t_k \leqslant T$. On the other hand, for the case $t_{k+1} - t_k = T$, which means that the system only needs to compute the optimal problem once at initial instant t_0, the real trajectory will converge into the robust terminal set where the state-feedback control law is applied. By Lemma 3, there is no need to prove the stability of the other case.

4.2 | Stability analysis

In this section, the stability of the closed-loop system is guaranteed by designing related parameters due to the uncertain disturbance and the event-triggered mechanism. The following theorem gives the stability analysis of the dual-mode control law.

Theorem 2. *For a class of continuous LTI systems with input constraints and bounded disturbances (1), suppose that all assumptions and Theorem 2 hold. If the system parameters satisfy*

$$\underline{\lambda}\left(\sqrt{Q}\right)^2 \sigma\varepsilon^2 - (r + \varepsilon)\bar{\lambda}\left(\sqrt{P}\right)^2 m\left[e^{aT} - e^{a(T-\sigma)}\right] - m^2\bar{\lambda}\left(\sqrt{Q}\right)^2 \mu - 2m\bar{\lambda}\left(\sqrt{Q}\right)^2 \varepsilon\sqrt{\left(\frac{T^2}{\sigma} - T\right)\mu} > 0, \tag{23}$$

where $\mu = \frac{1}{2a}(e^{2aT} - e^{2a\sigma}) - \frac{1}{a}(e^{2aT - a\sigma} - e^{a\sigma}) + \frac{1}{2a}(e^{2a(T-\sigma)} - 1)$. *Then, the system is practically stable and converges to the time-invariant region* Ω_γ.

Remark 5. In (23), the negative parts contain $m = \frac{\eta\|E\|}{\|A\|}$. Obviously, if the upper bound of disturbance satisfies $\eta = 0$, we easily get $\underline{\lambda}(\sqrt{Q})^2\sigma\varepsilon^2 \geqslant 0$. Thus, the stability is closely related to the disturbance compared with other parameters.

Proof. By the definition of the optimal function, we set $J(t_k, x^*(\tau|t_k), u^*(\tau|t_k))$ as the Lyapunov function $V(t_k)$ and we easily get $J(t_k, x^*(\tau|t_k), u^*(\tau|t_k)) \leqslant J(t_k, \bar{x}(\tau|t_k), \bar{u}(\tau|t_k))$ by suboptimality. The difference of the Lyapunov function at t_k and t_{k+1} is given by

$$\begin{aligned}\Delta V &= V(t_{k+1}) - V(t_k)\\ &= J(t_{k+1}, x^*, u^*) - J(t_k, x^*, u^*)\\ &\leqslant J(t_{k+1}, \bar{x}, \bar{u}) - J(t_k, x^*, u^*),\end{aligned} \tag{24}$$

where $\bar{u}(\tau|t_{k+1})$ is mentioned in (13).

To analyze stability more expediently, we partition ΔV into three parts, ie, $\Delta V = \sum_{i=1}^{3} \Delta V_i$, where

$$\begin{aligned}\Delta V_1 &= \int_{t_{k+1}}^{t_k+T} \left(\|\bar{x}(\tau|t_{k+1})\|_Q^2 - \|x^*(\tau|t_k)\|_Q^2\right) d\tau,\\ \Delta V_2 &= \int_{t_k+T}^{t_{k+1}+T} \left(\|\bar{x}(\tau|t_{k+1})\|_Q^2 + \|\bar{u}(\tau|t_{k+1})\|_R^2\right) d\tau + \|\bar{x}(t_{k+1}+T|t_{k+1})\|_P^2 - \|x^*(t_k+T|t_k)\|_P^2,\\ \Delta V_3 &= -\int_{t_k}^{t_{k+1}} \left(\|x^*(\tau|t_k)\|_Q^2 + \|u^*(\tau|t_k)\|_R^2\right) d\tau.\end{aligned}$$

We first suppose that $x(t_0) \notin \Omega_\varepsilon$ at initial instant.

For the first part, using the triangle inequality and (14), we transform the inequality as follows:

$$\begin{aligned}\Delta V_1 &\leqslant \int_{t_{k+1}}^{t_k+T} \left[\|\bar{x}(\tau|t_{k+1}) - x^*(\tau|t_k)\|_Q \left(\|\bar{x}(\tau|t_{k+1})\|_Q + \|x^*(\tau|t_k)\|_Q\right)\right] d\tau\\ &\leqslant \int_{t_{k+1}}^{t_k+T} \left[\|\bar{x}(\tau|t_{k+1})\|_Q + \|x^*(\tau|t_k)\|_Q\right] \left[\overline{\lambda}\left(\sqrt{Q}\right) \vartheta(\sigma) e^{\bar{\lambda}(A)(\tau - t_{k+1})}\right] d\tau.\end{aligned} \tag{25}$$

By the same reason, (14) can be rewritten as $\|\bar{x}(\tau|t_{k+1})\| \leqslant \|x^*(\tau|t_k)\| + \vartheta(\sigma) e^{\|A\|(\tau - t_{k+1})}$. Thus, substitute $\vartheta(\sigma) = me^{a\sigma} - m$ and integrate the right part of the last inequality of ΔV_1 except $\|x^*(\tau|t_k)\|$, then

$$\begin{aligned}\Delta V_1 \leqslant &\int_{t_{k+1}}^{t_k+T} 2m\overline{\lambda}\left(\sqrt{Q}\right)^2 \left[e^{a(\tau+\sigma-t_{k+1})} - e^{a(\tau-t_{k+1})}\right] \|x^*(\tau|t_k)\| \, d\tau\\ &+ m^2\overline{\lambda}\left(\sqrt{Q}\right)^2 \left[\frac{1}{2a}\left(e^{2aT} - e^{2a\sigma}\right) - \frac{1}{a}\left(e^{2aT-a\sigma} - e^{a\sigma}\right) + \frac{1}{2a}\left(e^{2a(T-\sigma)} - 1\right)\right].\end{aligned} \tag{26}$$

Applying the Hölder inequality to the integration with the part $\|x^*(\tau|t_k)\|$ and let $\mu = \frac{1}{2a}(e^{2aT} - e^{2a\sigma}) - \frac{1}{a}(e^{2aT-a\sigma} - e^{a\sigma}) + \frac{1}{2a}(e^{2a(T-\sigma)} - 1)$, it follows that

$$\begin{aligned}\Delta V_1 \leqslant &\left[\int_{t_{k+1}}^{t_k+T} 4m^2\overline{\lambda}\left(\sqrt{Q}\right)^4 (e^{2a(\tau+\sigma-t_{k+1})} - 2e^{(2a\tau+a\sigma-2at_{k+1})} + e^{2a(\tau-t_{k+1})}) d\tau\right]^{\frac{1}{2}} \cdot\\ &\left[\int_{t_{k+1}}^{t_k+T} \|x^*(\tau|t_k)\|^2 d\tau\right]^{\frac{1}{2}} + m^2\overline{\lambda}\left(\sqrt{Q}\right)^2 \mu,\end{aligned} \tag{27}$$

then considering the state constraint $\|x^*(\tau|t_k)\| \leqslant \frac{T\varepsilon}{\tau - t_k}$ and integrating the inequality, we have

$$\begin{aligned}\Delta V_1 &\leqslant 2m\overline{\lambda}\left(\sqrt{Q}\right)^2 \left[\mu \int_{t_{k+1}}^{t_k+T} \frac{T^2\varepsilon^2}{(\tau - t_k)^2} d\tau\right]^{\frac{1}{2}} + m^2\overline{\lambda}\left(\sqrt{Q}\right)^2 \mu\\ &\leqslant 2m\overline{\lambda}\left(\sqrt{Q}\right)^2 \varepsilon \sqrt{\left(\frac{T^2}{\sigma} - T\right)\mu} + m^2\overline{\lambda}\left(\sqrt{Q}\right)^2 \mu.\end{aligned} \tag{28}$$

For the second part, according to $\bar{u}(\tau|t_{k+1}) = K\bar{x}(\tau|t_{k+1})$, where $\tau \in [t_k + T, t_{k+1} + T]$, we integrate (12),

$$\int_{t_k+T}^{t_{k+1}+T} \left(\|\bar{x}(\tau|t_{k+1})\|_Q^2 + \|\bar{u}(\tau|t_{k+1})\|_R^2\right) d\tau \leqslant \|\bar{x}(t_k+T|t_{k+1})\|_P^2 - \|\bar{x}(t_{k+1}+T|t_{k+1})\|_P^2. \tag{29}$$

Substituting (29) into ΔV_2, we have

$$\begin{aligned}\Delta V_2 &\leqslant \|\bar{x}(t_k+T|t_{k+1})\|_P^2 - \|x^*(t_k+T|t_k)\|_P^2 \\ &\leqslant \overline{\lambda}\left(\sqrt{P}\right)^2 \|\bar{x}(t_k+T|t_{k+1}) - x^*(t_k+T|t_k)\| \cdot \\ &\quad (\|\bar{x}(t_k+T|t_{k+1})\| + \|x^*(t_k+T|t_k)\|)\,. \end{aligned} \tag{30}$$

Consider the state constraints $\|\bar{x}(t_k+T|t_{k+1})\| \leqslant r$ and $\|x^*(t_k+T|t_k)\| \leqslant \varepsilon$, then substitute (15) into (30) with $\tau = t_k + T$,

$$\begin{aligned}\Delta V_2 &\leqslant (r+\varepsilon)\overline{\lambda}\left(\sqrt{P}\right)^2 \vartheta(\sigma) e^{a(T-\sigma)} \\ &= (r+\varepsilon)\overline{\lambda}\left(\sqrt{P}\right)^2 m\left(e^{aT} - e^{a(T-\sigma)}\right). \end{aligned} \tag{31}$$

For the third part, note that $\|x^*(t_{k+1}|t_k)\| \leqslant \frac{T\varepsilon}{t_{k+1}-t_k}$ and $\frac{T\varepsilon}{t_{k+1}-t_k} \in \left[\varepsilon, \frac{T}{\sigma}\varepsilon\right]$, so

$$\begin{aligned}\Delta V_3 &= -\int_{t_k}^{t_{k+1}} \|x^*(\tau|t_k)\|_Q^2 + \|u^*(\tau|t_k)\|_R^2 \, d\tau \\ &\leqslant -\int_{t_k}^{t_{k+1}} \|x^*(\tau|t_k)\|_Q^2 \, d\tau \\ &\leqslant -\underline{\lambda}\left(\sqrt{Q}\right)^2 \sigma\varepsilon^2. \end{aligned} \tag{32}$$

Combine three parts by $\Delta V = \sum_{i=1}^{3} \Delta V_i$, and the Lyapunov function satisfies

$$\begin{aligned}\Delta V &\leqslant 2m\overline{\lambda}\left(\sqrt{Q}\right)^2 \varepsilon \sqrt{\left(\frac{T^2}{\sigma} - T\right)\mu} + m^2\overline{\lambda}\left(\sqrt{Q}\right)^2 \mu \\ &\quad + (r+\varepsilon)\overline{\lambda}\left(\sqrt{P}\right)^2 m\left(e^{aT} - e^{a(t-\sigma)}\right) + \left(-\underline{\lambda}\left(\sqrt{Q}\right)^2 \sigma\varepsilon^2\right) \\ &< 0. \end{aligned} \tag{33}$$

Therefore, if $\Delta V < 0$, we verify that $V(t_{k+1}) - V(t_k) < 0$ is tenable, which indicates that the real state trajectory will converge to the robust terminal set Ω_ε in finite time, ie, the real system is of practical stability. The proof of stability is completed. □

Remark 6. According to the proofs of the feasibility and the stability, the system parameters are closely related in the design process. A further initial state x_0 always requires a bigger control input or a longer prediction horizon, while the longer prediction horizon will accumulate the influence of the disturbances and increase the computational load. Particularly, due to the conservatism of the inequalities, Theorem 1 and Theorem 2 are sufficient conditions of the algorithm.

Remark 7. The triggering threshold value $\vartheta(\sigma)$ is closely related to control performance. Under the same disturbance, if we choose a longer inter-event time σ, computation can be sharply reduced at a cost that the control performance is lower. On the contrary, if σ is closer to $t_{k+1} - t_k$, the trajectory is similar to the optimal one and the event-triggered mechanism degrades to the periodic control.

5 | SIMULATION RESULTS

In this section, we apply the dual-mode control strategy to a 2-order LTI system to compare with the time-triggered one. In addition, the effects of the control strategy parameters are discussed in detail.

Consider a continuous LTI system as follows:

$$\dot{x}(t) = \begin{pmatrix} 2.5 & -1.75 \\ 0.8 & 0.1 \end{pmatrix} x(t) + \begin{pmatrix} 1 \\ -0.2 \end{pmatrix} u(t) + \begin{pmatrix} 0.5 \\ 0.5 \end{pmatrix} \omega, \tag{34}$$

where ω is a stochastic disturbance bounded by $\|\omega\| \leqslant \eta$. The initial state is set to be $x_0 = (0.851)^T$, and the input constraint is defined as $\|u(t)\| \leqslant 2$. First, we design the state-feedback gain according to Lemma 2 as $K = (-4.550.1)$. Then, the weight matrices in the optimization problem are chosen as $Q = \begin{pmatrix} 1.5 & 0 \\ 0 & 1.5 \end{pmatrix}$, $R = 0.1$ and $P = \begin{pmatrix} 1.2975 & -0.5301 \\ -0.5301 & 1.95 \end{pmatrix}$ satisfying Lemma 3.

For the time-triggered MPC, the prediction horizon is set to $T = 3.5$ seconds, the sampling time as $\Delta t = 0.05$ seconds and the whole simulation time as 10s. Then, we set the ETMPC with the same parameters as the traditional one. According to Theorem 1, the minimal inter-event time σ is bounded by $\sigma \geqslant 0.1356$ seconds and the upper bound of the disturbance is $\eta \leqslant 3.7 \times 10^{-3}$. We design the robust terminal region as $\Omega_\varepsilon = \{x | \|x(t)\| \leqslant 0.42\}$, ie, $\varepsilon = 0.42$. At last, we choose $\sigma = 0.2$ seconds and $\eta = 1.2 \times 10^{-3}$ to verify the stability from Theorem 2.

Figure 3 shows the difference of the state trajectories by the two control strategies. Figure 4 depicts the different control inputs. Supposing that the trajectory and the input computed by the time-triggered MPC are optimal, we can find that

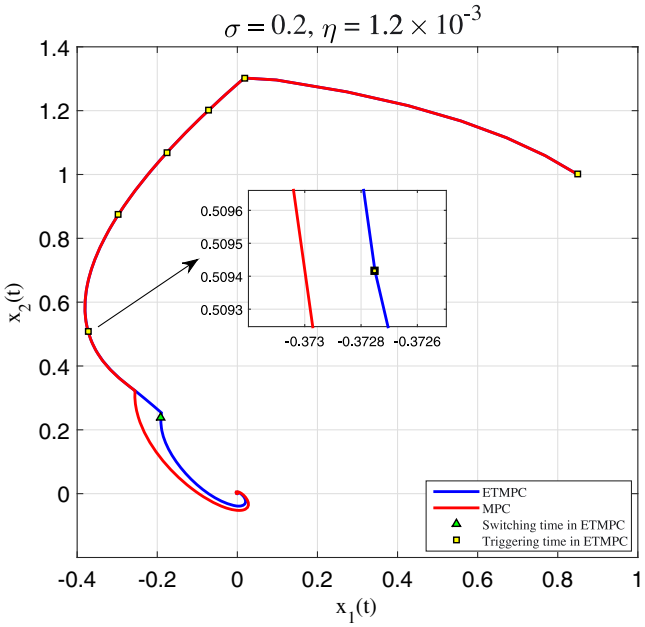

FIGURE 3 Comparison of the state trajectories. ETMPC, event-triggered model predictive control; MPC, model predictive control [Colour figure can be viewed at wileyonlinelibrary.com]

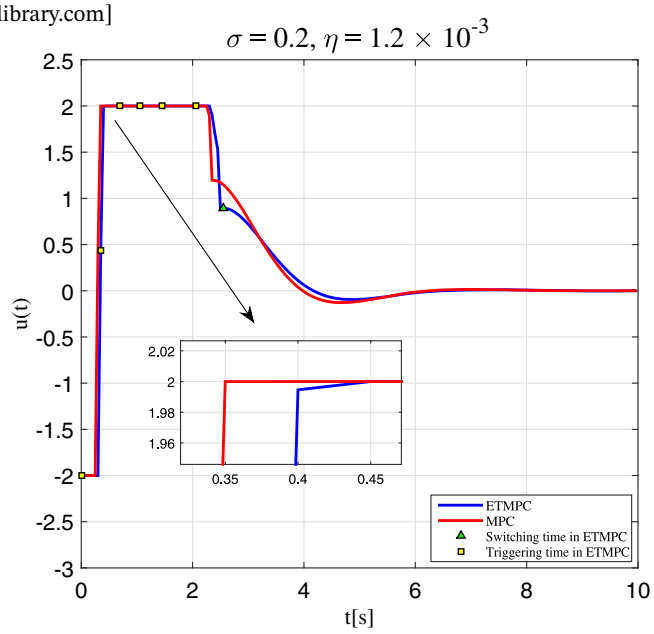

FIGURE 4 Comparison of the control inputs. ETMPC, event-triggered model predictive control; MPC, model predictive control [Colour figure can be viewed at wileyonlinelibrary.com]

the control performance and the control input of ETMPC are very similar to the time-triggered MPC. Before the two strategies switch to the state-feedback control law, the ETMPC solves the optimization problem only 6 times while the time-triggered MPC needs 46 times to enter the robust terminal region based on the same initial point. In conclusion, under the similar conditions and control performance, the ETMPC can reduce computation up to 86.96% in comparison with traditional MPC. When system states enter the robust terminal region, system close-loop stability and convergence precision are guaranteed by the state-feedback law and the upper bound of disturbance.

Because the inter-event time σ and the upper bound of disturbance η are the most essential parameters in event-triggered strategy, we compare the state trajectory and control input with three sets of parameters. Figure 5A and Figure 5C are the simulation results of the same system with $\sigma = 0.4$ seconds and $\eta = 1.2 \times 10^{-3}$. Compared with Figure 3 and Figure 4, the optimization problem is solved only 3 times, which is less than a half of the simulation with $\sigma = 0.2$ seconds and cause the control performance worse. Furthermore, under the bound $\eta = 1.2 \times 10^{-3}$ of disturbance, the longer inter-event time σ indicates greater tolerance to the same disturbance.

Figure 5B and Figure 5D show the state trajectory and the control input with parameters $\sigma = 0.2$ seconds and $\eta = 0.6 \times 10^{-3}$. The control performance is the best one of the three sets of parameters due to the smallest σ and η. Based on the above three results, we can find that the inter-event time σ is the main impact factor on control performance rather than the amplitude of disturbance. The computation is 50% when σ is reduced by half from Figure 3 and Figure 5A while disturbance does not matter much according to Figure 3 and Figure 5B.

By implementing four sets of comparable parameters, Figure 6 shows the Euclidean distance of the state trajectories by the ETMPC and time-triggered MPC at each triggering time and each point represents the corresponding triggering moment. It can be easily verified that, as the inter-event time σ increasing, computation is decreased observably while the deviation from the optimal trajectory is greater. On the other hand, a larger disturbance causes triggering time to arrive earlier but has a smaller impact on control performance compared with σ.

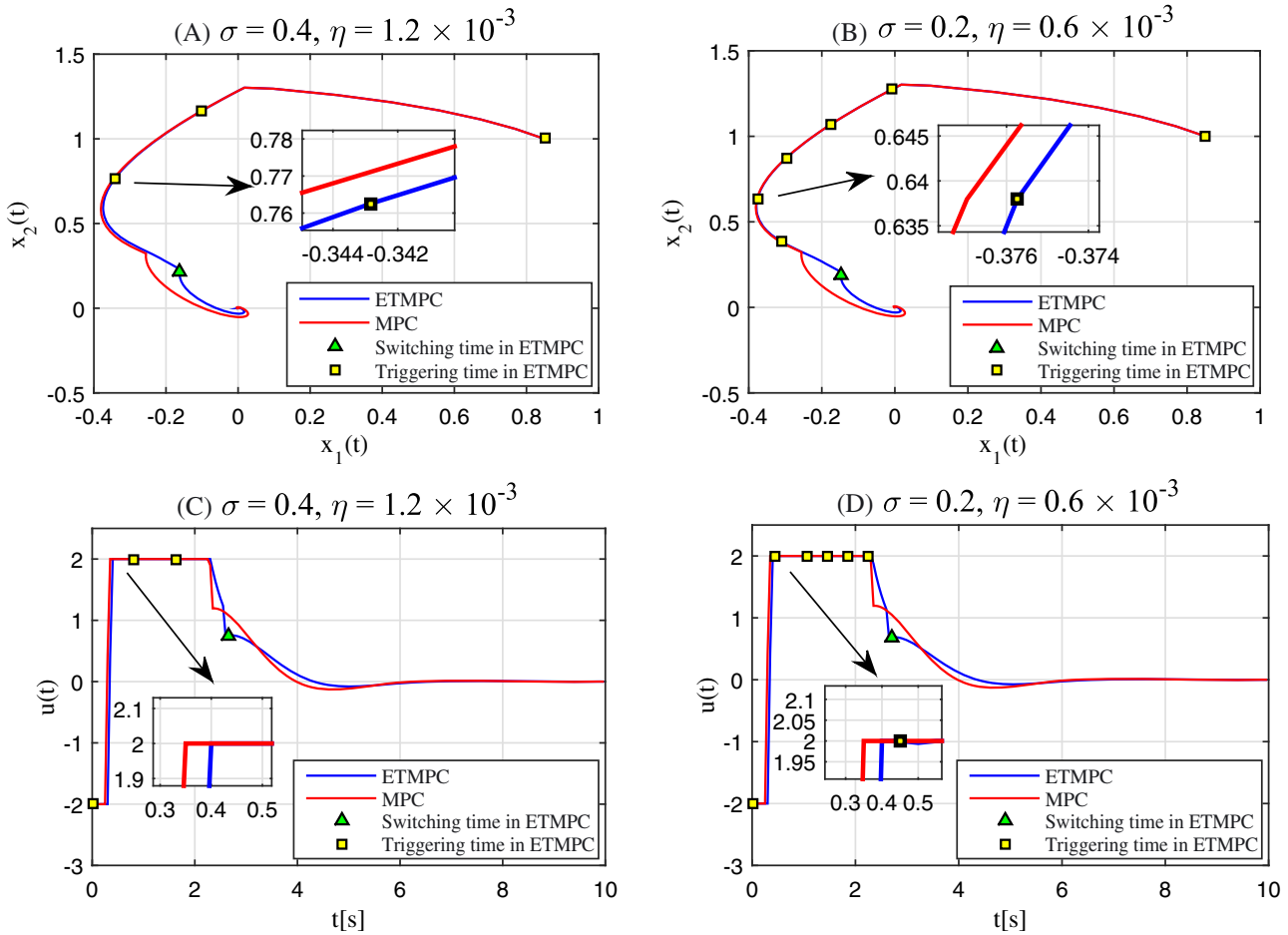

FIGURE 5 Comparison of the control performance using event-triggered model predictive control (ETMPC) with two sets of parameters and time-triggered model predictive control (MPC). A, $\sigma = 0.4, \eta = 1.2 \times 10^{-3}$; B, $\sigma = 0.2, \eta = 0.6 \times 10^{-3}$; C, $\sigma = 0.4, \eta = 1.2 \times 10^{-3}$; D, $\sigma = 0.2, \eta = 0.6 \times 10^{-3}$ [Colour figure can be viewed at wileyonlinelibrary.com]

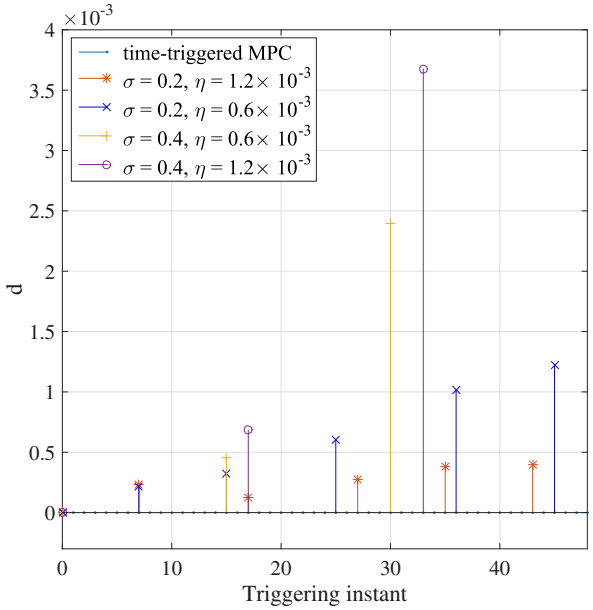

FIGURE 6 The triggering instant and the difference of state trajectories by different strategies. MPC, model predictive control [Colour figure can be viewed at wileyonlinelibrary.com]

In conclusion, the simulation shows the difference of the traditional MPC and the ETMPC by four sets of parameters. First, computational load is reduced at least 80% by implementing event-triggered mechanism and control performance has no significant degradation. Second, compared with the disturbances, the inter-event time σ has a greater influence in ETMPC. At last, under the same inter-event time σ, a stronger disturbance causes a shorter interval of solving the optimization problem.

6 | CONCLUSION

In this paper, a dual-mode strategy based on ETMPC and state-feedback control law for a class of continuous LTI systems with input constraints and bounded disturbances has been developed to reduce computational load and ensure control performance. Then, we designed the system parameters to guarantee recursive feasibility and stability. Specifically, we discussed the importance of the inter-event time and the upper bound of the disturbances in detail for the event-triggered mechanism by numerical simulation and comparison. In general, the strategy strikes a balance between computational load and control performance. Future research will aim at reducing the conservatism and improving the robustness of the system.

ACKNOWLEDGEMENTS

The work was supported by the Beijing Natural Science Foundation under Grant 4161001, the National Natural Science Foundation under Grant 61836001 and 61803033, the National Natural Science Foundation Projects of International Cooperation and Exchanges under Grant 61720106010, the Foundation for Innovative Research Groups of the National Natural Science Foundation of China under Grant 61621063.

ORCID

Yuanqing Xia https://orcid.org/0000-0002-5977-4911

REFERENCES

1. Mayne DQ. Model predictive control: recent developments and future promise. *Automatica*. 2014;50(12):2967-2986.
2. Mayne DQ, Rawlings JB, Rao CV, Scokaert PO. Constrained model predictive control: stability and optimality. *Automatica*. 2000;36(6):789-814.
3. Fleming J, Kouvaritakis B, Cannon M. Robust tube MPC for linear systems with multiplicative uncertainty. *IEEE Trans Autom Control*. 2015;60(4):1087-1092.

4. Bumroongsri P, Duangsri S. Robust model predictive control of linear time-varying systems with bounded disturbances. *Int J Chem Eng Appl*. 2014;5(3):210.
5. Maciejowski JM. *Predictive Control: With Constraints*. London, UK: Pearson Education; 2002.
6. Rawlings JB, Mayne DQ. *Model Predictive Control: Theory and Design*. San Francisco, CA: Nob Hill Pub; 2009.
7. Lehmann D, Henriksson E, Johansson KH. Event-triggered model predictive control of discrete-time linear systems subject to disturbances. In: Proceedings of European Control Conference; 2013; Zurich, Switzerland.
8. Bemporad A, Morari M. Robust model predictive control: a survey. In: *Robustness in Identification and Control*. London, UK: Springer; 1999:207-226.
9. Limon D, Alvarado I, Alamo T, Camacho E. Robust tube-based MPC for tracking of constrained linear systems with additive disturbances. *J Process Control*. 2010;20(3):248-260.
10. Betti G, Farina M, Scattolini R. A robust MPC algorithm for offset-free tracking of constant reference signals. *IEEE Trans Autom Control*. 2013;58(9):2394-2400.
11. Alvarado I, Limón D, Alamo T, Camacho EF. Output feedback robust tube based MPC for tracking of piece-wise constant references. Paper presented at: 2007 46th IEEE Conference on Decision and Control; 2007; New Orleans, LA.
12. Ding B, Xi Y, Cychowski MT, OMahony T. Improving off-line approach to robust MPC based-on nominal performance cost. *Automatica*. 2007;43(1):158-163.
13. Marruedo DL, Alamo T, Camacho E. Input-to-state stable MPC for constrained discrete-time nonlinear systems with bounded additive uncertainties. In: Proceedings of the 41st IEEE Conference on Decision and Control, vol. 4; 2002; Las Vegas, NV.
14. Heemels W, Johansson KH, Tabuada P. An introduction to event-triggered and self-triggered control. Paper presented at: 2012 IEEE 51st IEEE Conference on Decision and Control (CDC); 2012; Maui, HI.
15. Tabuada P. Event-triggered real-time scheduling of stabilizing control tasks. *IEEE Trans Autom Control*. 2007;52(9):1680-1685.
16. Dimarogonas DV, Johansson KH. Event-triggered control for multi-agent systems. In: Proceedings of the IEEE Conference on Decision and Control; 2009; Shanghai, China.
17. Lunze J, Lehmann D. A state-feedback approach to event-based control. *Automatica*. 2010;46(1):211-215.
18. Heemels W, Donkers M. Model-based periodic event-triggered control for linear systems. *Automatica*. 2013;49(3):698-711.
19. Sun Z, Dai L, Xia Y, Liu K. Event-based model predictive tracking control of nonholonomic systems with coupled input constraint and bounded disturbances. *IEEE Trans Autom Control*. 2018;63(2):608-615.
20. Brunner FD, Heemels W, Allgower F. Robust event-triggered MPC with guaranteed asymptotic bound and average sampling rate. *IEEE Trans Autom Control*. 2017;62(11):5694-5709.
21. Darup MS, Dyrska R, König K, Monnigmann M. A novel event-triggered robust MPC scheme for linear systems. Paper presented at: 2017 IEEE 56th Annual Conference on Decision and Control (CDC); 2017; Melbourne, Australia.
22. Ferrara A, Oleari AN, Sacone S, Siri S. An event-triggered model predictive control scheme for freeway systems. Paper presented at: 2012 IEEE 51st IEEE Conference on Decision and Control (CDC); 2012; Maui, HI.
23. Brunner FD, Heemels W, Allgöwer F. Robust event-triggered MPC for constrained linear discrete-time systems with guaranteed average sampling rate. *IFAC-Pap*. 2015;48(23):117-122.
24. Li H, Shi Y. Event-triggered robust model predictive control of continuous-time nonlinear systems. *Automatica*. 2014;50(5):1507-1513.
25. Berglind JB, Gommans T, Heemels W. Self-triggered MPC for constrained linear systems and quadratic costs. *IFAC Proc Vol*. 2012;45(17):342-348.
26. Gommans T, Heemels W. Resource-aware MPC for constrained nonlinear systems: a self-triggered control approach. *Syst Control Lett*. 2015;79:59-67.
27. Brunner FD, Heemels M, Allgöwer F. Robust self-triggered MPC for constrained linear systems: a tube-based approach. *Automatica*. 2016;72:73-83.
28. Liu C, Li H, Gao J, Xu D. Robust self-triggered min-max model predictive control for discrete-time nonlinear systems. *Automatica*. 2018;89:333-339.
29. Hashimoto K, Adachi S, Dimarogonas DV. Self-triggered model predictive control for nonlinear input-affine dynamical systems via adaptive control samples selection. *IEEE Trans Autom Control*. 2017;62(1):177-189.
30. Dunbar WB. Distributed receding horizon control of dynamically coupled nonlinear systems. *IEEE Trans Autom Control*. 2007;52(7):1249-1263.
31. Zadeh LA, Deoser CA. *Linear System Theory*. Huntington, NY: Robert E Krieger Publishing Company Huntington; 1976.
32. Li H, Shi Y. Robust distributed model predictive control of constrained continuous-time nonlinear systems: a robustness constraint approach. *IEEE Trans Autom Control*. 2014;59(6):1673-1678.
33. Khalil HK, Grizzle J. *Nonlinear Systems*. Vol. 3. Upper Saddle River, NJ: Prentice Hall; 2002.

How to cite this article: Luo Y, Xia Y, Sun Z. Robust event-triggered model predictive control for constrained linear continuous system. *Int J Robust Nonlinear Control*. 2018;1–14. https://doi.org/10.1002/rnc.4432